Hybrid Block Coordinate Optimization for 3-D Cooperative UAV Sensing and Communication

Inpyo Lee† and Jasung Lim†
†Department of Military Digital Convergence, Ajou University, Suwon, South Korea
Email: {andy224079@, jaslim@}ajou.ac.kr

Abstract— This paper addresses mission-time minimization in multi-UAV sensing-and-communication for wide-area monitoring. Each rotary-wing UAV can vary its altitude as well as its planar path, and the sensing load is split into one common and several individual tasks to balance duration against on-board energy. The resulting non-convex 3-D planning problem is solved by a lightweight two-stage hybrid block-coordinate algorithm: task ratios and transmit powers are refined via a polyblock search, while each UAV's altitude is updated through a one-dimensional golden-section scan. Simulations show that exploiting the vertical degree of freedom shortens mission time by 6–8 % relative to 2-D baselines with only modest computation.

Index Terms—Multi-UAV cooperation, altitude control, block-coordinate algorithm, cooperative sensing & communication

I. INTRODUCTION

Airborne sensing with unmanned aerial vehicles (UAVs) has attracted intense interest for disaster relief, smart agriculture, and traffic monitoring, owing to its ability to bypass terrain obstructions and be rapidly dispatched to target areas. [1], [2]. When multiple UAVs operate cooperatively, sensing and backhaul latency can be reduced, while virtual–array transmission improves link reliability [3]. Existing approaches include relay-based communication, which reduces latency [4], [5] but sacrifices sensing efficiency and introduces additional noise and delay, and distributed multi-antenna cooperative transmission, which enhances communication performance [6], [7], [8] but requires explicit data sharing among UAVs before transmission, leading to extra time and energy

In multi-UAV sensing and transmission (S&T) systems, adaptive task allocation can further shorten mission time by exploiting UAV mobility to flexibly assign workloads [9], [10], [11]. Conventional non-overlapping strategies maximize coverage but result in UAVs holding disjoint data, which prevents the formation of a virtual multi-antenna system for cooperative transmission. This limitation motivates task-allocation frameworks that intentionally allow partial data overlap to gain cooperative communication benefits without sacrificing sensing efficiency.

Meng et al. proposed the *Joint Task Allocation and Power Optimization* (JTAPO) framework, which optimizes task ratios and transmit powers for a set of common and individual sensing

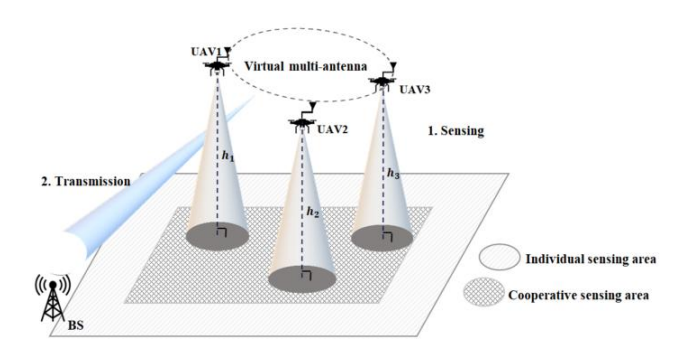


Fig. 1. System model of multi-UAV performing S&T tasks.

tasks [12]. Although JTAPO improves energy efficiency by combining workload partitioning with virtual MISO transmission, it still (i) assumes a fixed-altitude 2-D trajectory, forfeiting potential 3-D benefits, and (ii) relies on a full polyblock search for global optimization, which becomes expensive as the number of UAVs grows.

In this paper, we propose mission-time minimization for a 3-D cooperative S&T system in which M rotary-wing UAVs execute one common and M individual tasks. The formulated mixed-integer nonlinear program jointly optimizes discrete altitude levels, task-allocation ratios, and transmit powers under per-UAV energy constraints. To solve this problem, we propose a hybrid block-coordinate descent (BCD) framework that combines polyblock outer approximation for the task-power block with a one-dimensional golden-section search for each UAV's altitude. Unlike existing 2-D schemes such as JTAPO, the proposed algorithm satisfies the exact BCD conditions of Beck and Tetruashvili [13] and guarantees global optimality. Simulation results demonstrate that our method reduces overall mission time by 6-8% compared with state-of-the-art 2-D benchmarks, underscoring the practical value of exploiting vertical freedom in real-time multi-UAV operations.

II. System Model

As shown in Fig. 1, we consider a time-division multi-UAV uplink where M UAVs, indexed by $m \in \mathcal{M} = \{1, ..., M\}$ cooperatively sense a ground region and forward the gathered data to a single ground BS. Distinct from prior works that restrict UAVs to fixed altitudes or purely horizontal trajectories, our model explicitly includes the altitude h_m as part of the UA state. Each UAV moves at speed v and transmits the collected data from $X_m = [x_m, y_m, h_m]$ to a BS located at origin (0, 0, 0).

This work was supported by the National Research Foundation of Korea(NRF) grant funded by the Korea government(MSIT) (N0. 2021R1A2C2007112).

A. Task Division

Let the area to be sensed by UAVs be A, and the total sensed data be C. Each UAV is assigned one common task and M individual tasks. Let the proportion of the common task be ω_0 , and the task ratio for the ω_m , which satisfy:

$$\sum_{m=0}^{M} \omega_m = 1 \tag{1}$$

$$0 \le \omega_m \le 1, \forall m \in \mathcal{M} \cup \{0\}$$
 (2)

B. Sensing Model

While the UAV flies at speed v, the time T_m^s required for UAV m to sense its allocated region is given by:

$$T_m^s = (\omega_0 + \omega_m) A \frac{\Delta t}{v \cdot GSD_{ref} \cdot R_{sens}}, \ GSD_{ref} = \frac{h_m \cdot p}{f}$$
 (3)

Where $(\omega_0 + \omega_m)A$ represents the area sensed by UAV m, Δt denotes the time of shutter interval, GSD_{ref} is the ground sampling distance, and R_{sens} indicates the sensor resolution, p denotes the pixel size of the camera, and f represents the focal length of the camera lens[14].

C. Wireless Channel Model

Assuming the UAV-to-BS link exhibits a line-of-sight (LoS) probability greater than 90 % at operational altitudes (\geq 20 m) and short horizontal distances (\leq 300 m) according to 3GPP TR 38.901, the channel's large-scale power gain γ_m is modeled using the free-space path loss (FSPL) and neglect small-scale fading and log-normal shadowing:

$$\gamma_m = \left[\frac{c}{4\pi df\sigma}\right]^2 \tag{4}$$

Where $d = \sqrt{x_m^2 + y_m^2 + h_m^2}$ is the distance from BS to UAV m, f is the carrier, σ the antenna gain factor, and c the speed of light.

D. Transmission Delay

1) Individual transmission phase

Assuming adaptive modulation coding that operates near the Shannon limit, the achievable rate for UAV m is $R_m = B \log_2(1 + p_m^i \gamma_m(h_m))$, With $p_m^i \le p_{max}$ the transmit power, B the system bandwidth and $C\omega_m$ the individual transmit data. The individual-phase transmission time (T_m^{ti}) is modeled by dividing the transmit data by the achievable rate:

$$T_m^{i} = \frac{C\omega_m}{B\log_2(1+p_m^{i}\gamma_m)} \tag{5}$$

2) Cooperative transmission phase

During the cooperative phase the M time-synchronised UAVs simultaneously forward the common-task payload to the BS, thereby forming a virtual MISO uplink [6]. Because the signals add coherently at the receiver, the effective SNR is the sum of the individual SNRs, $\sum_{i=1}^{M} p_i^{tc} \gamma_i(h_i)$, Under this model the cooperative-phase transmission time becomes

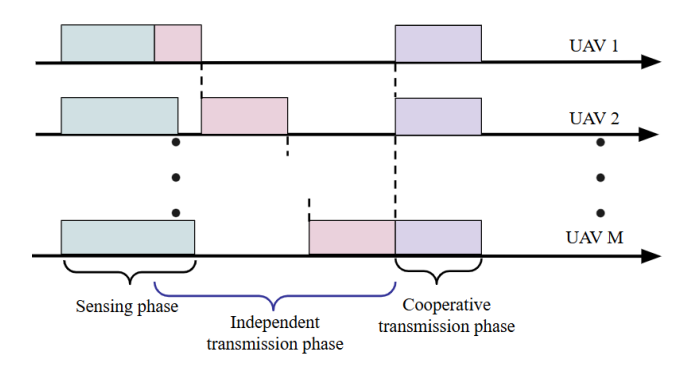


Fig. 2. Timeline of proposed multi-UAV sensing-tranmission protocol

$$T^{c} = \frac{c\omega_{0}}{B\log_{2}(1+\sum_{m=1}^{M}p_{m}^{c}\gamma_{m})}$$
 (6)

E. Energy Budget

The total onboard energy of a rotary-wing UAV is dominated by propulsion; however, propulsion power is largely independent of the task-power variables (ω, p) and nearly constant within our 60–120 m altitude band. Hence we prebudget a fixed communication share of the battery and enforce the transmit-energy constraint

$$E_m = p_m^{i} T_m^{i} + p_m^{c} T^{c} \le \bar{E}, \ \forall m \in \mathcal{M}$$
 (7)

$$0 \le p_m^c \le p^{max}, \ 0 \le p_m^i \le p^{max}, \forall m \in \mathcal{M}$$
 (8)

Where p_m^i and p_m^c the transmit powers that UAV m dedicates to its individual and cooperative phases and \bar{E} represents the available energy reserve. In addition, both power variables are capped by the hardware-limited peak value p^{max} :

F. Mission-completion time

As illustrated in Fig. 2, after completing its assigned sensing task, the UAV that finishes first immediately begins its individual uplink transmission to the BS. Individual transmissions are multiplexed by TDMA, such that UAV m+1 can start its uplink only after UAV m has completed its own slot, thereby avoiding interference among independent links. Once every UAV has finished its TDMA interval, all M UAVs synchronously enter the cooperative-transmission phase, where identical common-task data is jointly transmitted using virtual—array beamforming to maximize link reliability. The mission-completion time is given by:

$$T = T_1^s + \sum_{m=1}^M T_m^i + T^c$$
 (9)

Because the channel is released only after the current TDMA slot finishes, the following causality constraint must hold:

$$T_m^{max} + T_m^i \ge T_{m+1}^s \tag{10}$$

With T_m^{max} denoting the latest instant at which UAV m is still occupying the channel.

TABLE I. THREE BLOCKS

Block	Variables	Key structure	Exact solver
B1-task ratio	ω	Monotone (normal set)	Polyblock
B2-Power	p^i , p^c	Quasi-convex fractional	1-D bisection + SCS
B3-Altitude	h	Unimodel	Golden search

III. PROPOSED HYBIRD BLOCK-COORIDINATE ALGORIGM

The Hybrid Block-Coordinate (BCD) scheme solves Problem (P0) to global optimality while keeping the polyblock burden low.

$$(P0): \min_{\omega, p^i, p^c h} T$$
s. t. (1), (2), (7), (8), (10) (12)

T is the total mission time; ω contains the task-allocation ratios, p^i , p^c are the individual and cooperative power vectors, and h the altitude vector. Constraints (1), (2) specify sensing and transmission models; (7), (8) impose the per-UAV energy and peak-power limits, and (10) enforces the TDMA causality.

A. Block Decompostion

We divide (P0) into three blocks. Blocks B1 and B2 are designed to optimize the task ratio and transmission power, respectively, based on the approach proposed by Meng et al., while Block B3 optimizes the UAV altitude using the Golden search method introduced by Kiefer[15].

Golden-Search is an iterative method for finding the global minimum of a unimodal function by repeatedly dividing the search interval according to the golden ratio, approximately 0.618. Empirical results show that setting $\varepsilon = 10^{-3}$, allows the optimal altitude for each UAV to be identified within 6 to 8 iterations.

B. Hybrid-BCD Procedure

The proposed Hybrid BCD procedure (see Algorithm 1) initializes every UAV altitude to the mid-point and sets the task-ratio and power vectors to uniform values, then executes the following two-stage outer loop. Stage 1 performs N_p Polyblock updates on the joint block (ω, p) , exploiting the monotone structure to move these variables toward their global minimizer. Stage 2 refines each altitude h_m in parallel via a one-dimensional Golden-section search, which yields an ε_h -exact optimum. The loop terminates when the relative mission-time reduction $\Delta T/T$ falls below a preset threshold ε the resulting triple (ω^*, p^*, h^*) .

C. Exactness of the BCD Updates

This subsection proves that each block in Algorithm 1 is solved exactly—that is, every update attains the global minimizer of the block-wise sub-problem of (P0). The result ensures that the outer Block—Coordinate iterations converge to a globally optimal solution of (P0).

Lemma 1 (Block B1&B2 exactness) With h fixed, the mission time is strictly monotone—decreasing when any task ratio is reduced or any transmit power is increased—while the corresponding task—power feasibility set is downward-closed (normal). A monotone programme over a normal set admits a polyblock outer-approximation that converges to the unique global optimum. Hence the inner loop in Blocks B1–B2 always returns the globally optimal task split and power allocation for the current altitudes.

Lemma 2 (Block B3 exactness) With (ω, p) fixed, the altitude-related cost $J_m(h)$ for each UAV m can be expressed as follows.

$$J_{m}(h) = \underbrace{\kappa \frac{(\omega_{0} + \omega_{m}) \cdot A}{h_{m}}}_{optional} + \underbrace{\frac{C\omega_{m}}{B \log_{2} \left(1 + p_{m}^{i} \gamma_{m}(h_{m})\right)}}_{\frac{C\omega_{0}}{B \log_{2} \left(1 + \sum_{i=1}^{M} p_{i}^{c} \gamma_{i}(h_{i})\right)}}$$
(13)

When the sensing term is present, $J_m(h)$ exhibits a unimodal structure and admits a unique global minimum within the interior of the feasible region. If the sensing term is absent and the cost function is strictly increasing, then the global minimum is attained at h_{min} In both cases, the structure satisfies the quasi-block property, ensuring that applying the Golden Section Search guarantees convergence to the global optimum.

D. Convergence Guarantee

The proposed algorithm can be globally updated for (ω, p, h) using three distinct blocks: (a) Polyblock (b) 1-D bisection and (c) Golden Search. This framework satisfies all conditions of the exact BCD theorem proposed by Beck and Tetruashvili[13]:

- (i) Each block domain forms a compact Cartesian product set;
- (ii) The mission time T is a continuous and lower-bounded function.
- (iii) All blocks are invoked infinitely often in a bounded-cycle manner with exact minimization.

Therefore, the iterative sequence $x^k = (\omega^k, p^k, H^k)$ satisfies $T(x^{k+1}) \le T(x^k)$, $x^{(k)} \to x$ *. Empirical evaluations confirm that with $\varepsilon = 10^{(-2)}$, the total mission time error remains below 0.1%.

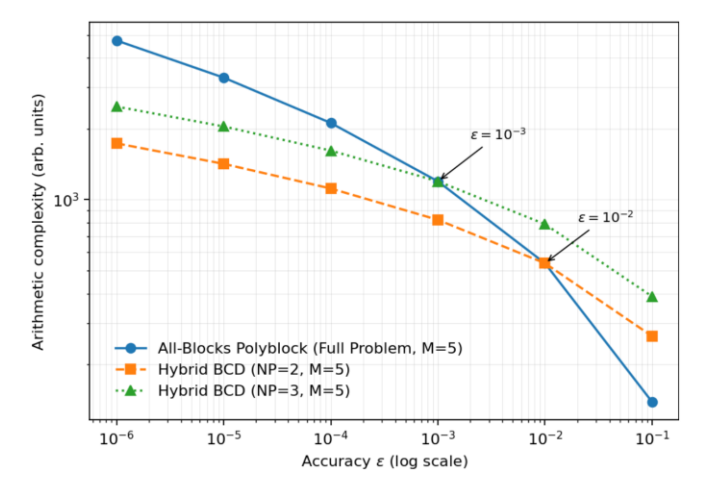


Fig. 3. Complexity with Accuracy: All-Blocks Polyblock vs Hybrid BCD

E. Computation Complexity

For Blocks B1•B2, the polyblock method solves a monotonic program with 3M+1 decision variables (task ratios and power allocations). Each projection onto the feasible set involves solving a convex program of complexity $\mathcal{O}(M^3)$, and the outer polyblock iterations require N_p steps for accuracy ϵ . Thus, the total complexity of this stage scales as

$$\mathcal{O}(N_p \cdot M^3) \tag{14}$$

Where N_p is the number of polyblock updates. In the case of a full polyblock search without N_p -budgeting, the overall complexity scales as $\mathcal{O}(\log(1/\epsilon) \cdot M^3)$. As shown in Fig. 3, the proposed HBC method becomes advantageous when the required accuracy ϵ is smaller than 1.0×10^{-2} . For Block B3, each UAV's altitude is refined via golden-section search. As the altitude-related cost is unimodal, the optimum can be located within $\mathcal{O}(\log((H_{max} - H_{min})/\epsilon))$ evaluations per UAV. Since this process runs in parallel with all UAVs, the total cost is

$$\mathcal{O}(M \cdot \log((H_{max} - H_{min})/\epsilon)) \tag{15}$$

Combining both stages, the overall complexity of the proposed HBC framework is

$$\mathcal{O}\left(log(1/\epsilon)\cdot(N_p\cdot M^3 + log\frac{H_{max}-H_{min}}{\epsilon}\cdot M)\right) \quad (16)$$

which grows polynomially in fleet size M and only logarithmically in accuracy. This ensures scalability compared with the full polyblock search in [12], whose exponential dependence on dimension becomes prohibitive for large UAVs.

IV. SIMULATION RESULTS

We simulate a 1e6 m² sensing area. The default fleet is M = 3 whose horizontal positions are uniformly sampled; all sensing/communication parameters are following Table II. For

TABLE II. DE FAULT PARAMETER

Parameter	Symbol	Default Value
Number of UAVs	М	3
Sensing Area	A	$1.0 \times 10^6 m^2$
Total sensed data	С	150Mb
Bandwidth	B	1MHz
Max Tx power	$p_n^{(max)}$	10nW
Energy buddget	E	0.1MJ
Numerical accuracy	ϵ	1.0×10^{-6}
Altitude search range	$[H_{min}, H_{max}]$	60-120m
Shutter interval	Δt	0.5s
Sensor resolution	R_{sens}	20MP
Pixel size	p	4.4μm
Focal length	f	10mm
Ployblock loop iteration	N_p	2

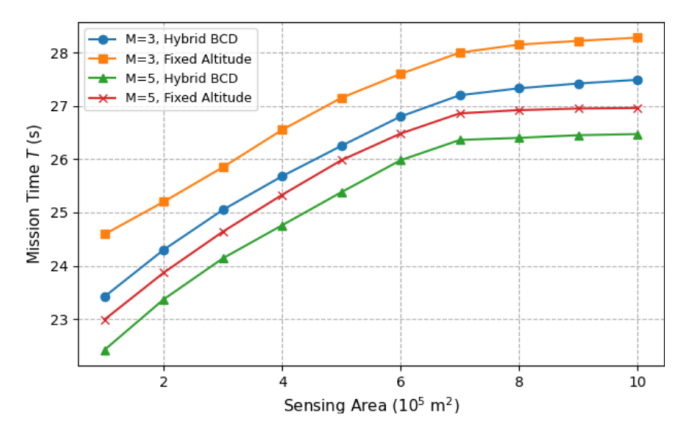


Fig. 4. Mission Time vs Sensing Area for Different UAV Numbers

intuition: with pixel size $p = 4.4\mu m$ and focal length f = 10mm, the ground sampling distance at h = 100m is GSD = 4.4cm/pixel

A. Impact of UAV numbers and Altitude Control

Fig. 4 plots the mission completion time versus the sensing area for two fleet sizes (M = 3,5) under the Hybrid BCD and fixed-altitude(JTAPO) schemes. Increasing the number of UAVs from M = 3 to M = 5 reduces the mission time, since the sensing workload per UAV decreases and the cooperative transmission gain improves. Although mission time grows with the sensing area in all cases, the Hybrid BCD maintains a consistent performance gap over the fixed-altitude baseline, demonstrating robustness across different operation scales.

B. Impact of Polyblock Updates on Convergence of Mission Time

Per outer iteration, the Hybrid BCD runs B1•B2 via polyblock (budget N_p), and B3 altitudes via golden-section search. Fig. 5 shows mission time versus outer iteration for $M \in \{3,5\}$ and $N_p \in \{2,3\}$. All curves exhibit an L-shaped drop: most improvement occurs in the first 1–2 iterations, then the trajectories flatten. Increasing N_p mainly speeds up the early drop without changing the final level, and the larger fleet consistently attains a lower T due to smaller per-UAV sensing

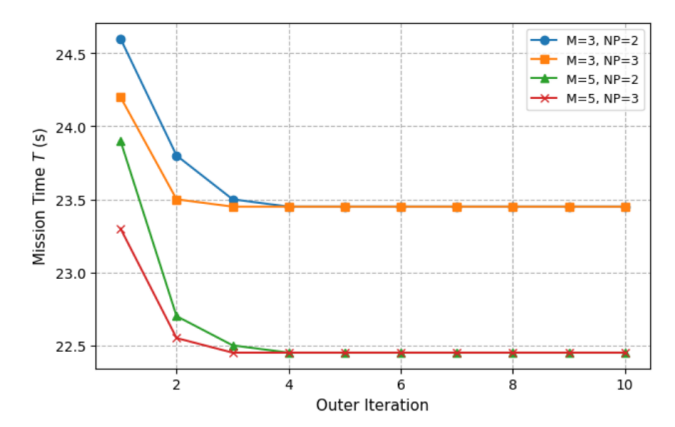


Fig. 5. Mission Time Convergence versus Outer Iteration for Different M and N_p

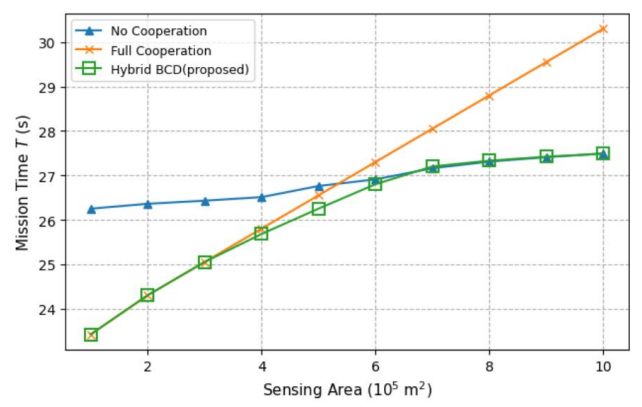


Fig. 6. Mission Time vs Sensing Area for Different UAV Numbers

load and stronger cooperative sum-SNR. The method stabilizes within \sim 3 outer iterations, so modest N_p suffices. This validates the efficiency of the block decomposition, which achieves near-optimal performance with limited computational overhead.

C. Sensitivity to Sensing Area

Fig. 6 summarizes the mission time under three strategies (i) Hybrid BCD (proposed), (ii) No Cooperation ($\omega_0=0$), and (iii) Full Cooperation ($\omega_0=1$) while sweeping the sensing area and the available energy. When the target area expands from $1\times 10^5 {\rm m}^2$ to $1\times 10^6 {\rm m}^2$, the mission time of all schemes grows with area size, but the trends differ. No Cooperation avoids redundancy yet suffers from limited transmission gain, while Full Cooperation incurs severe duplication, making it inefficient for large areas. In contrast, Hybrid BCD balances task partitioning and cooperative transmission, yielding consistently lower mission times and robust scalability.

IV. CONCULSION

This paper proposed a Hybrid Block-Coordinate (BCD) algorithm for 3-D multi-UAV sensing and communication. A three-block design—task ratio (polyblock), power (1-D bisection), and altitude (golden search)—achieves global optimality with low complexity.

Per-iteration cost is $\mathcal{O}(N_p \cdot M^3)$ for B1–B2 plus $\mathcal{O}(\log((H_{max} - H_{min})/\epsilon \cdot M))$ for B3, so accuracy enters only logarithmically; in practice the algorithm converges in 2–4 outer iterations for $N_p \in \{2,3\}$. On our benchmarks, altitude optimization (Block B3) alone shortens mission time by 6–8% versus fixed-height JTAPO, and adaptive cooperation (variable ω_0) yields up to an additional 20% reduction when energy is ample. With per-UAV kernels parallelized, wall-clock runtime grows near-linearly with fleet size and remains tractable beyond (M=5). These results confirm that vertical control and flexible task overlap are key to real-time aerial sensing. Future work will address distributed implementations, joint trajectory—hovering optimization, and online adaptation to time-varying LoS conditions.

REFERENCES

- [1] Y. Zeng, R. Zhang, and T. J. Lim, "Wireless communications with unmanned aerial vehicles: Opportunities and challenges," *IEEE Commun. Mag.*, vol. 54, no. 5, pp. 36–42, May 2016.
- [2] C. Zhan, Y. Zeng, and R. Zhang, "Energy-efficient data collection in UAV enabled wireless sensor network," *IEEE Wireless Commun. Lett.*, vol. 7, no. 3, pp. 328–331, Jun. 2018.
- [3] Q. Wu, Y. Zeng, and R. Zhang, "Joint trajectory and communication design for multi-UAV enabled wireless networks," *IEEE Trans. Wireless Commun.*, vol. 17, no. 3, pp. 2109–2121, Mar. 2018.
- [4] S. Zhang, H. Zhang, B. Di, and L. Song, "Cellular UAV-to-X communications: Design and optimization for multi-UAV networks," *IEEE Trans Wireless Commun.*, vol. 18, no. 2, pp. 1346–1359, Feb. 2019.
- [5] J. Scherer and B. Rinner, "Multi-UAV surveillance with minimum information idleness and latency constraints," *IEEE Robot. Autom. Lett.* 5, no. 3, pp. 4812–4819, Jul. 2020.
- [6] M. N. Soorki, M. H. Manshaei, B. Maham, and H. Saidi, "On uplink virtual MIMO with device relaying cooperation enforcement in 5G networks," *IEEE Trans. Mobile Comput.*, vol. 17, no. 1, pp. 155–168, Jan. 2018
- [7] Q. Wu, Y. Zeng, and R. Zhang, "Joint trajectory and communication design for multi-UAV enabled wireless networks," *IEEE Trans. Wireless Commun.*, vol. 17, no. 3, pp. 2109–2121, Mar. 2018.
- [8] C. You and R. Zhang, "3D trajectory optimization in Rician fading for UAV-enabled data harvesting," *IEEE Trans. Wireless Commun.*, vol. 18, no. 6, pp. 3192–3207, Jun. 2019.
- [9] X. Chen, Z. Feng, Z. Wei, F. Gao, and X. Yuan, "Performance of jointsensing-communication cooperative sensing UAV network," *IEEE Trans. Veh. Technol.*, vol. 69, no. 12, pp. 15545–15556, Dec. 2020.
- [10] H. Menouar, I. Guvenc, K. Akkaya, A. S. Uluagac, A. Kadri, and A. Tuncer, "UAV-enabled intelligent transportation systems for the smart city: Applications and challenges," *IEEE Commun. Mag.*, vol. 55, no. 3, pp. 22–28, Mar. 2017.
- [11] Y. Zeng and R. Zhang, "Energy-efficient UAV communication with trajectory optimization," *IEEE Trans. Wireless Commun.*, vol. 16, no. 6, pp. 3747–3760, Jun. 2017.
- [12] K. Meng, X. He, Q. Wu, and D. Li, "Multi-UAV Collaborative Sensing and Communication: Joint Task Allocation and Power Optimization," *IEEE Trans. Wireless Commun.*, vol. 22, no. 6, pp.4232–4246, Dec. 2022.
- [13] A. Beck and L. Tetruashvili, "On the convergence of block coordinate descent type methods," *SIAM Journal on Optimization*, vol. 23, no. 4, pp. 2037–2060, 2013.
- [14] B. Li, Q. Li, Y. Zeng, Y. Rong, and R. Zhang, "3-D Trajectory Optimization for Energy-Efficient UAV Communication: A Control Design Perspective," *IEEE Trans. Wireless Commun.*, vol. 21, no. 6, pp. 4579–4594, Jun. 2022.
- [15] J. Kiefer, "Sequential minimax search for a maximum," Proceedings of the American Mathematical Society, vol. 4, no. 3, pp. 502–506, Jun. 1953.